



ARTICLE

A Bifunctional Brønsted Acidic Deep Eutectic Solvent to Dissolve and Catalyze the Depolymerization of Alkali Lignin

Lifen Li¹, Zhigang Wu¹, Xuedong Xi², Baoyu Liu³, Yan Cao³, Hailong Xu³ and Yingcheng Hu^{4,*}

¹College of Forestry, Guizhou University, Guiyang, 550025, China

²ENSTIB-LERMAB, University of Lorraine, Epinal, 88051, France

³Special and Key Laboratory for Development and Utilization of Guizhou Superior Bio-Based Materials, Guizhou Minzu University, Guiyang, 550025, China

⁴Key Laboratory of Bio-Based Material Science and Technology of Ministry of Education of China, College of Material Science and Engineering, Northeast Forestry University, Harbin, 150040, China

*Corresponding Author: Yingcheng Hu. Email: yingchenghu@163.com

Received: 15 June 2020 Accepted: 03 August 2020

ABSTRACT

Lignin is an abundant renewable macromolecular material in nature, and degradation of lignin to improve its hydroxyl content is the key to its efficient use. Alkali lignin (AL) was treated with Brønsted acidic deep eutectic solvent (DES) based on choline chloride and *p*-toluenesulfonic acid at mild reaction temperature, the structure of the lignin before and after degradation, as well as the composition of small molecules of lignin were analyzed in order to investigate the chemical structure changes of lignin with DES treatment, and the degradation mechanism of lignin in this acidic DES was elucidated in this work. FTIR and NMR analyses demonstrated the selective cleavage of the lignin ether linkages in the degradation process, which was in line with the increased content of phenolic hydroxyl species. XPS revealed that the O/C atomic ratio of the regenerated lignin was lower than that of the AL sample, revealing that the lignin underwent decarbonylation during the DES treatment. Regenerated lignin with low molecular weight and narrow polydispersity index was obtained, and the average molecular weight (M_w) decreased from 17680 g/mol to 2792 g/mol (130°C, 3 h) according to GPC analysis. The lignin-degraded products were mainly G-type phenolics and ketones, and small number of aldehydes were also generated, the possible degradation pathway of lignin in this acidic DES was proposed.

KEYWORDS

Alkali lignin; depolymerization; Brønsted acidic deep eutectic solvent; structural analysis

1 Introduction

Lignin is a complex three-dimensional amorphous polymer composed of phenylpropane structural units randomly linked by ether bonds or carbon-carbon bonds; 45–50% and 60–62% of the structural units in softwood and hardwood lignin are connected by β -O-4 bonds [1]. The global production of lignin was estimated at 100 million tonnes/year in 2015, but only less than 2% has achieved highly efficient utilization because of the complex composition, structural heterogeneity, and low reactivity of lignin [2]. The degradation of lignin by appropriate methods was considered one of the most important challenges in



lignin utilization by reducing the dispersibility of lignin, and afford lignin fragments with lower molecular weights, higher activities, and more homogeneous physical and chemical properties [3]. Degraded lignin can be used to partly replace phenol and formaldehyde to synthesize phenolic resin, partly replace bisphenol A and epichlorohydrin to synthesize epoxy resin, or as a substitute for polyether polyols and polyisocyanate to prepare lignin-based polyurethane foams [4,5]. Traditional lignin degradation methods include alkali catalysis, acid catalysis, metal catalysis and supercritical fluid-assisted degradation, but harsh treatment conditions are required (usually $>300^{\circ}\text{C}$, 10 MPa), and biodegradation treatment takes a long time (usually several days) [6].

In recent years, deep eutectic solvents (DESs) have attracted extensive attention as a medium to effectively fractionate lignocellulosic material to dissociate lignin and improve the enzymatic hydrolysis rate of cellulosic materials due to their special properties, such as simple preparation, renewability, and excellent solubility of lignin, and they are promising alternatives to ILs in biomass processes [7]. Choline chloride (ChCl)-lactic acid was considered a suitable DES for biomass pretreatment, for example, the delignification rate of rice straw was 60.0% at 60°C for 12 h with ChCl-lactic acid (1:5), 27.8% with 0.5% NaOH at room temperature for 24 h, and 10.0% with 1.5% H_2SO_4 at 121°C for 60 min [8]. However, acylation, condensation, and depolymerization of lignin occurred during ChCl-lactic acid pretreatment [9]. Hong et al. [10] investigated the chemical transformations of the ChCl-lactic acid lignin by 2D-HSQC NMR spectroscopy and found that acylation occurred between the γ -OH groups in the lignin and the COOH groups in the lactic acid.

Chen et al. [11] found that ChCl and *p*-toluenesulfonic acid (*p*-TsOH) could rapidly form Brønsted acidic DES by heating at a molar ratio of 1:1, and this solvent could be used as a hydrogen bond donor and catalyst for the dehydration of fructose [12]. Recently, Wang et al. [13] fractionated wheat straw and miscanthus using a Brønsted acidic DES consisting of ChCl and *p*-TsOH at low temperature and compared the extracted lignin with that obtained with *p*-TsOH/ H_2O . They found that the H^+ concentration in the ChCl-*p*-TsOH system was lower than that in the aqueous *p*-TsOH/ H_2O system, and the addition of ChCl facilitated lignin dissolution and decreased lignin condensation. At 80°C for 20 min, the delignification rate was 76.6% for miscanthus and 88.9% for straw with DES consisting of 75% *p*-TsOH and 25% ChCl.

In the present work, the degradation of alkali lignin (AL) was performed using ChCl-*p*-TsOH (1:1, molar ratio), a Brønsted acidic DES, as both the solvent and catalyst. The aim of this work was to analysis the chemical structures changes of lignin and to elucidate mechanism of lignin degradation in this acidic DES. The chemical structure and thermal properties of lignin before and after degradation were evaluated by spectroscopy (FTIR, ^1H NMR, HSQC-NMR, XPS), GPC and TG analyses, and the small-molecule products from the degradation of lignin were analyzed by GC-MS. Furthermore, the possible degradation pathways of lignin in this acidic DES were proposed, which provides a foundation for further research and utilization of lignin.

2 Materials and Methods

2.1 Materials

Choline chloride (ChCl, $\text{C}_5\text{H}_{14}\text{ClNO}$, $>98\%$), *p*-toluenesulfonic acid monohydrate (*p*-TsOH, $\text{C}_7\text{H}_8\text{O}_3\text{S}\cdot\text{H}_2\text{O}$, $>98.5\%$) and alkali lignin (AL) were purchased from Sigma-Aldrich and dried under vacuum at 60°C for 24 h before used. The other chemicals obtained from commercial suppliers were of analytical grade and were used as received.

2.2 Synthesis of DES

ChCl and *p*-TsOH were mixed at a mole ratio of 1:1 and stirred at 100°C for approximately 40 min, resulting in a colorless liquid, and then stored in a desiccator until use.

2.3 Experimental Procedures

The typical procedure for lignin degradation was as follows. Approximately 1 g of AL was dissolved in 20 g of DES, yielding a lignin concentration of 5 wt%, and then 250 μ L of distilled water was added. The degradation reactions were carried out at 130°C in sealed vials for set times. Once the reaction time had elapsed, the reaction flask was immediately transferred into a cold water bath to stop the reaction. Then, lignin was precipitated from the reaction mixture by adding 100 mL of distilled water. After centrifugation, the solid residue was thoroughly washed with 150 mL of water, and the regenerated lignin was dried at 80°C for 12 h to a constant weight. The regenerated lignin samples were labeled L₁, L₃, L₅ and L₁₂ for 1, 3, 5 and 12 h degradation at 130°C, and the recovery yield (wt%) of L₁, L₃, L₅ and L₁₂ was 95.7%, 93.8%, 89.3% and 88.7%, respectively. Collected the supernatant, and then removed water by rotary evaporation, finally the DES can be recovered and reused. The schematic diagram of experimental process was shown in Fig. 1.

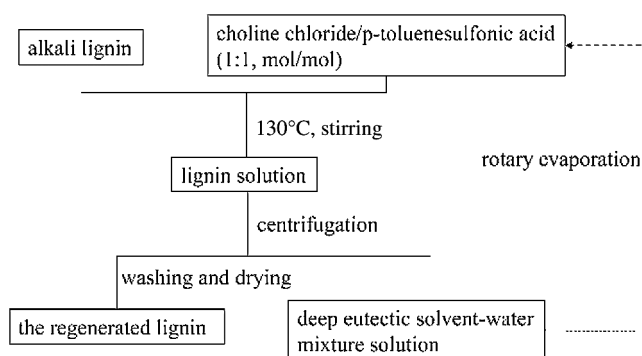


Figure 1: The scheme of degradation of lignin in deep eutectic solvent

2.4 Product Analysis

2.4.1 FT-IR Spectroscopy

The FTIR spectra of the lignin samples were recorded with a Fourier transform infrared spectrophotometer (Nicolet 6700, Thermo Fisher Scientific, USA) within the wavelength range of 4000–500 cm^{-1} at 4 cm^{-1} resolution.

2.4.2 Two-Dimensional NMR Spectroscopy

2D ^{13}C - ^1H HSQC (heteronuclear single quantum correlation) spectra were acquired at room temperature on a Bruker 500 MHz spectrometer. A lignin sample (approximately 80 mg) was dissolved in 0.5 mL of dimethyl sulfoxide ($\text{DMSO}-d_6$). The spectral widths for the ^1H and ^{13}C dimensions were 10,000 Hz and 30,000 Hz, respectively. The conditions for the hydrogen spectrum acquisition were as follows: 32 scans and a relaxation delay time of 1 s. The acquisition conditions for the carbon spectrum were 28569 scans and a relaxation delay time of 2 s.

2.4.3 Gel Permeation Chromatography (GPC)

The molecular weight and distribution of the lignin samples were determined by gel permeation chromatography (Agilent 1100, USA) with a JASCO UV-1575 detector at 254 nm and a tandem system of two columns (79911GP-101 and 79911GP-104). The concentration of lignin in tetrahydrofuran (THF)

was approximately 5 mg/mL. The column temperature was 30°C, and THF was used as the eluent with a flow rate of 1 mL/min. The average molecular weight of the lignin was measured through an external standard method wherein monodisperse polystyrene was applied as a standard compound.

2.4.4 Thermal Properties

The thermal properties of lignin before and after degradation were determined with a thermogravimetric analyzer (PerkinElmer, STA 6000). The heating rate was 10°C/min, the range of heating was 40–800°C, and the flow rate of high purity N₂ was 20 mL/min.

2.4.5 GC-MS Analysis

The small molecule degradation products of the lignin were analyzed by gas chromatography-mass spectrometry with an Agilent instrument (789 NA/7000B). An HP-5MS column was used (30 m × 0.25 mm × 0.25 μm). The injection volume was 1 μL, the split ratio was 20:1, the carrier gas was helium, and the flow rate was 1.0 mL/min. The column temperature was kept at 40°C for 5 min, increased to 280°C at a rate of 10°C/min, and held at 280°C for 10 min. The peaks were assigned based on comparison to the mass spectrometry library of the National Institute of Standards and Technology (NIST, 2005).

3 Results and Discussion

3.1 Infrared Spectrum Analysis of the Regenerated Lignin

FTIR spectroscopy was used to characterize the functional groups changes of lignin during the acidic DES treatment, and Fig. 2 compares the FTIR spectra of the lignin samples regenerated at 130°C for different times. The broad band around 3305 cm⁻¹ was assigned to stretching vibrations of lignin's phenolic and aliphatic hydroxyl group, which increased in intensity and redshifted with increasing reaction time. The peak at 2928 cm⁻¹ was attributed to C-H stretching vibration of -CH₃ and -CH₂, which showed little change in peak intensity. The absorption band at 1697 cm⁻¹ typically represented C=O stretching vibrations in ketone or aldehyde groups, peak at 1156 cm⁻¹ corresponds to the conjugated ester-based C=O stretching vibration, and the intensity of these two peaks showed a slight increase first and then decrease with elongated treated time. Reasonable speculation is that ketone compounds had been formed, implying that the lignin underwent a partial oxidation reaction during treatment with ChCl-*p*-TsOH. In addition to oxidized lignin structure, the destruction of carbonyl and carboxyl groups may also take place with prolonged reaction time. Which supported previous studies that oxidation of the C_α alcohol to ketone was crucial to promote the cleavage of the β-O-4 linkages, while the destruction of the conjugated carbonyl structure is the most prevalent mechanism of lignin depolymerization during acidic pretreatment [10,14,15]. The peaks at 1600 cm⁻¹ and 1502 cm⁻¹, assigned to the vibration of the aromatic ring skeleton, remained almost unchanged, indicating that the aromatic structures were preserved during the reaction. Signals at 1078 cm⁻¹ corresponded to the C-O deformation of secondary alcohols and aliphatic esters, which monotonically decreased with increasing reaction time. According to the method of Fox et al. [16], comparing the absorbances of the characteristic lignin peaks with that of the characteristic benzene ring peak at 1502 cm⁻¹ at different treatment times, the change in the functional group content in the lignin can be semiquantitatively analyzed. The ratio of the intensities at 3305 cm⁻¹ and 1078 cm⁻¹ can be used to estimate the relative contents of hydroxy group and ether bond in the regenerated lignin, and the results are shown in Fig. 3. The ratio values of A₃₃₀₅/A₁₅₀₂ gradually increased with the extension of treatment time, while that of A₁₀₇₈/A₁₅₀₂ decreased sharply with the duration of time, implying the cleavage of the lignin ether linkages during acid-catalyzed degradation and the concomitant formation of hydroxyl groups [9,17]. Overall, the FTIR spectra indicated obvious changes of the chemical structure of lignin taking place during the DES treatment, and the longer reaction times were favorable for the complete cleavage of the lignin ether linkages.

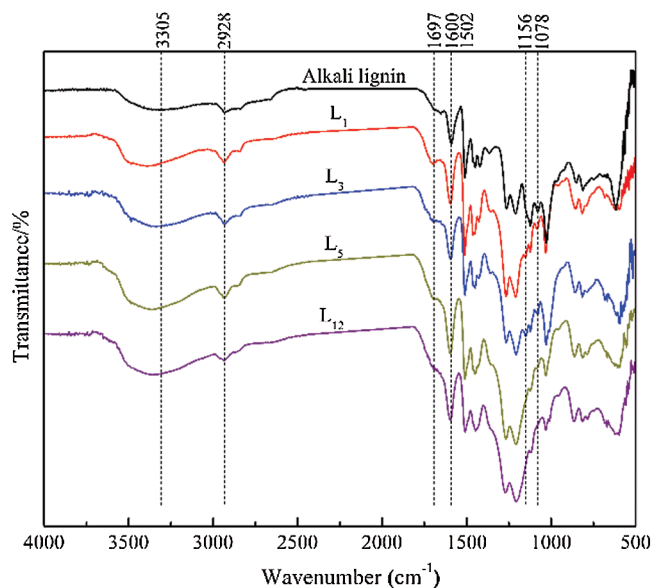


Figure 2: FTIR spectra of AL and the regenerated lignins

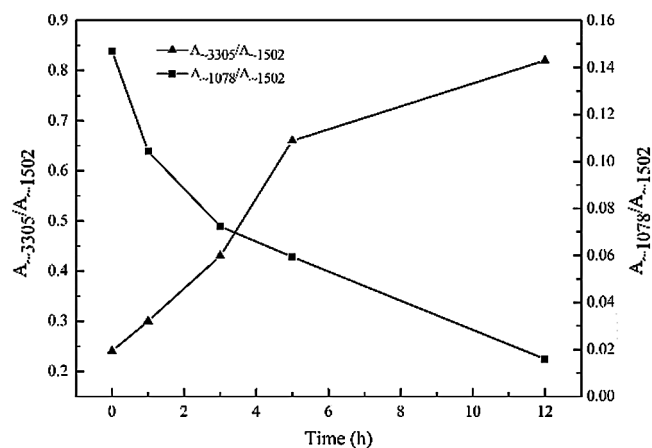


Figure 3: Ratio of the absorbance intensities of different FTIR bands to that of 1502 cm^{-1} vs. degradation time

3.2 Hydrogen Spectrum Analysis of the Regenerated Lignin

The ^1H NMR spectra of lignin acylated for different degradation times are shown in Fig. 4. The signals from 8.0 to 6.2 ppm belong to the aromatic protons in the guaiacyl (G) units and syringyl (S) units, the signals from 5.0 to 4.1 ppm belong to the H_α , H_β and H_γ signals in the structure of $\beta\text{-O-4}$, those from 4.1 to 3.5 ppm are the methoxy proton signals, and the peaks at 3.5–3.3 ppm are the proton signals of water in the solvent. The small peak at 3.4 ppm is the proton signal from CHCl_3 , and the appearance of this peak may be due to the slight reaction between lignin and CHCl_3 during the degradation or a small amount of CHCl_3 remaining in the regenerated lignin. The peak at 2.5 ppm is attributed to the nondeuterated DMSO. The signals from 2.5 to 2.2 ppm belong to the protons of the aromatic acetates, and those from 2.2 to 1.4 ppm belong to the protons of aliphatic acetates. The intensity of the acetate signal of lignin was significantly increased after degradation. According to the literature [18], the methoxy group can be used as a standard peak to analyze the number of protons in each functional group of lignin, as shown in Fig. 5. As we can see, the phenol hydroxyl content

increased significantly with the extension of the lignin degradation time, which was nearly two times higher than that of AL, while the alcohol hydroxyl content did not significantly change with time. Since the cleavage of the β -O-4 bond will form new phenolic hydroxyl groups, while the cleavage of the C_{α} - C_{β} bonds will increase the content of alcohol hydroxy groups in the lignin [19], implying that cleavage of the β -O-4 ether bonds is the main reaction of lignin in this acidic DES. According to previous literatures, lignin with abundant hydroxyl groups has a high reactivity toward formaldehyde and dimethylamine, besides, the antioxidant activity is closely related to the amount of the phenolic hydroxyl groups of lignin [20,21]. Thus, the regenerated lignin with a high phenolic hydroxy group content is expected to be a biobased material suitable for producing high-value polymers, such as lignin-based phenolic resin and antioxidants, etc.

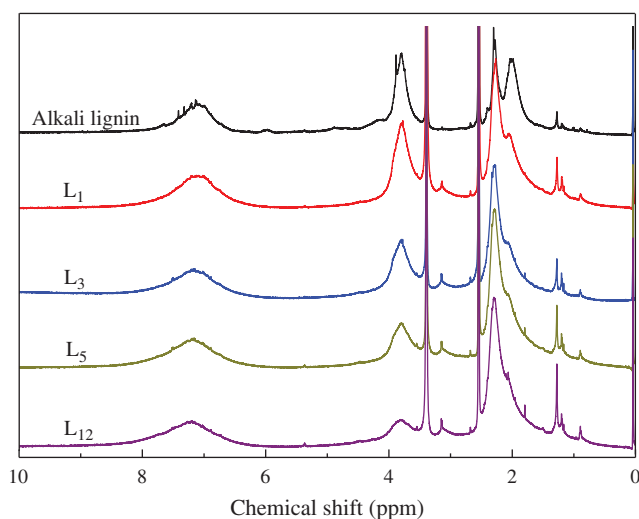


Figure 4: ^1H NMR spectra of AL and the regenerated lignins

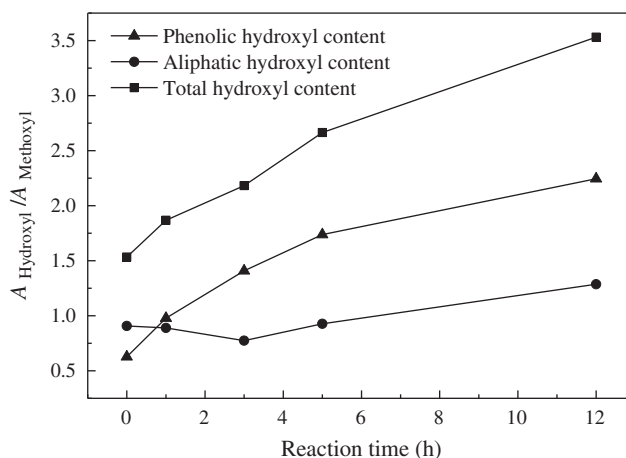


Figure 5: Ratio of the areas of the hydroxy and methoxy peaks *versus* degradation time

3.3 Two-Dimensional NMR Analysis of the Regenerated Lignin

Two-dimensional (2D) heteronuclear single-quantum correlation (HSQC) nuclear magnetic resonance (NMR) spectroscopy can provide qualitative and quantitative information on the basic structural units (G, S, and H) of lignin as well as the connection modes between the units based on the carbon-hydrogen

correlation signals in the lignin structure. Fig. 6 shows the HSQC spectra of AL (left) and L₅ (right). The assignments of the C-H correlations in the spectra are shown in Tab. 1, and a schematic of the basic connection units and structural units is shown in Fig. 7.

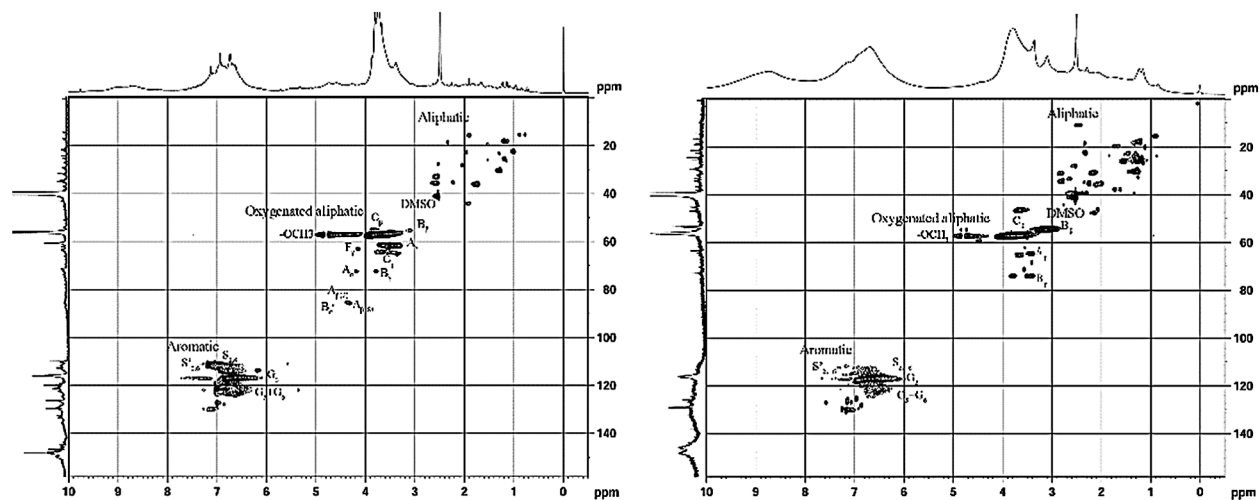


Figure 6: 2D HSQC NMR spectra of AL (left) and the degraded lignin (right)

Table 1: Assignments of the ¹³C-¹H correlation signals in the HSQC spectrum of AL

Number	Signal assignment
C _β	C _β -H _β of phenylcoumarin unit (C)
B _β	C _β -H _β of β-β resin alcohol unit (B)
-OCH ₃	C-H in methoxy group
A _γ	C _γ -H _γ in the structure (A) of β-O-4
F _γ	C _γ -H _γ of terminal group of <i>p</i> -hydroxy cinnamyl alcohol (F)
C _γ	C _γ -H _γ of phenyl coumarin unit (C)
B _γ	C _γ -H _γ of β-β resin alcohol unit (B)
A _α	C _α -H _α in the structure (A) of β-O-4
A _β (G)	C _β -H _β in the β-O-4 (A) connecting G unit
B _α	C _α -H _α of β-β resin alcohol unit (B)
A _β (S)	C _β -H _β in the β-O-4 (A) connecting S unit
S _{2,6}	Etherified syringyl units (S), C _{2,6} -H _{2,6}
S' _{2,6}	Oxidized syringyl unit (S'), C _{2,6} -H _{2,6}
G ₂	C ₂ -H ₂ of guaiacol unit (G)
G ₅	C ₅ -H ₅ of guaiacol unit (G)
G ₆	C ₆ -H ₆ of guaiacol unit (G)

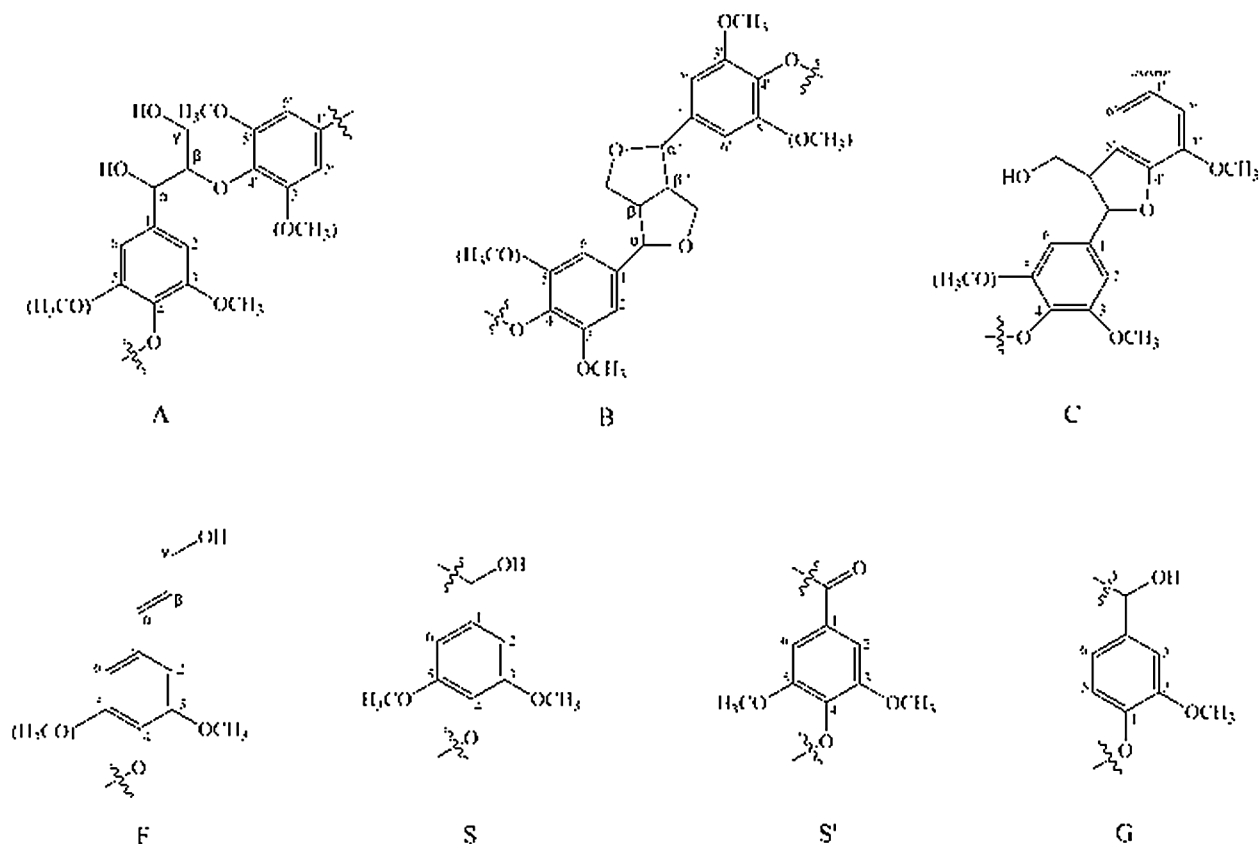


Figure 7: Main initial and acetylated substructures involving different side-chain linkages and aromatic units identified from the 2D NMR spectra of AL: (A) β -O-4 aryl ether linkages with a free-OH at the γ -carbon; (B) resinol substructures formed by β - β' , α -O- γ and γ -O- α linkages; (C) phenylcoumarin substructures formed by β -5 and α -O-4 linkages; (F) *p*-hydroxycinnamyl alcohol end groups; (S) syringyl unit; (S') oxidized syringyl units with a C_α ketone; (G) and guaiacyl unit

The 2D-HSQC spectrum of lignin can be divided into three regions: the aliphatic side chain region (δ_C/δ_H 40~10/2.5~0.5 ppm), the oxidized aliphatic region (δ_C/δ_H 95~50/6.0~2.5 ppm) and the aromatic ring region (δ_C/δ_H 135~100/8.0~5.0 ppm). Among these regions, the oxidized aliphatic regions includes the signals characteristic of the linking modes between the lignin macromonomers, and the β -O-4 ether bond was the most abundant interunit linkage detected, including C_α - H_α , C_β - H_β and C_γ - H_γ on β -O-4 (A). In addition to the β -O-4 chemical bonds, the hydrocarbon-coupled signals of C_α - H_α , C_β - H_β , C_γ - H_γ in the β - β' resin alcohol unit (B), C_β - H_β and C_γ - H_γ in the phenyl coumarin unit (C) and C_γ - H_γ in the end group of hydroxycinnamol (F) were also detected. In the AL material, the signals of the $A_{\beta(G)}$ and $A_{\beta(S)}$ bond structures were obvious, but these signals had basically disappeared in the spectrum of L_5 , which proves that the ether bond was cleaved in the regenerated lignin. Cleavage of β -O-4 linkages of lignin extracted with *p*-TsOH from poplar wood was also found in earlier published research [22].

Analyzing the change of the S/G (syringyl/guaiacyl) ratio is helpful for evaluating the structure changes of lignin. According to the calculation method in reference [23], ^{13}C NMR spectroscopy can be used to analyze the S/G unit ratio in lignin. The quantitative method was as follows: S/G was half of the peak area integral of $S_{2,6}$ divided by the G_2 peak area integral, where the $S_{2,6}$ signal was integrated from 108.9 to 101.0 ppm, and the G_2 signal was integrated from 113.0 to 110.0 ppm. According to this method, the S/G value of AL was 0.81, while that of L_5 was 1.88. Some studies [15] have suggested that the S-type

lignin unit in acidic solvents can easily remove methoxy groups, which leads to an increase in the content of G-type lignin units, therefore, the S/G value of lignin after treatment in acidic solvents decreases. However, in this research, the S/G value of lignin increased after degradation, it was reasonable to deduce that the increase in S/G value was caused because G-type units were preferentially degraded in this acidic DES than S-type unit, and the condensation reaction took place preferably at G units than S units under acidic conditions, through the free C5 or C6 position, which lead to an increase in the S/G ratio [24]. This phenomenon was in line with the previous literature [13], which showed that S/G ratio of lignin increased with fractionation severity of herbaceous biomass during CHCl_3 -*p*-TsOH treatment. On the other hand, further analysis of the degree of polymerization (DP) before and after lignin degradation showed that the DP of AL was 2.09, while that of L₅ was 2.35, indicating that condensation reaction took place during treatment with the acidic DES.

3.4 Surface Analysis of Lignin by XPS Valence Band Spectra

X-ray photoelectron spectroscopy (XPS) measurements were carried out to obtain information about the elemental composition and valence states. There are four C1s valence states on the lignin surface, namely, C1, C2, C3 and C4, which represent different carbon-carbon bonds on the lignin surface, and their electronic binding energies correspond to different functional groups in the lignin. The proportions of C1-C4 in the C1s peak could be expressed by the percentage of the peak area. There are two kinds of valence states of lignin O1s, O1 and O2. O1 corresponds to oxygen atoms in oxygen-carbon single bonds, such as C-OH and C-O-C, O2 corresponds to oxygen atoms in carbon-oxygen double bonds, including the oxygen atoms in aldehydes, ketones, esters and carbonyls (C=O and O-C=O).

The C1s and O1s signals of the regenerated lignin samples treated with this acidic DES for different times were subjected to curve fitting and peaking, and the XPS spectra of carbon and oxygen were obtained (Fig. 8). The results of the oxygen-carbon atom ratio in the lignin and the ratios of the peak areas are listed in Tab. 2. The O/C atom ratio in the lignin treated with DES decreased, and the relative content of the C1 peak increased, which may be due to the increase in the contents of hydrocarbons or carbon-carbon single bonds, and the relative content of the C3 peak notably decreased, we presumed that the proportion of C and O atoms in the combined form was reduced. After degradation, the relative content of O1 in the lignin increased significantly, while the relative content of O2 decreased significantly, it was reasonable to deduce that the decrease in relative content of O2 was caused by decarbonylation reaction.

Table 2: Atomic O/C ratios and C1s and O1s peak deconvolution of the original and degraded lignins

Sample	O/C (%)	C1 (%)	C2 (%)	C3 (%)	C4 (%)	O1 (%)	O2 (%)
		C-C C-H	C-O	O-C-O C=O	O-C=O	C-OH C-O-C	C=O COOR
AL	40.79	57.71	26.74	12.56	2.98	38.42	61.58
L ₁	31.99	67.00	27.89	3.77	1.34	53.82	46.18
L ₃	27.92	71.54	22.64	4.67	1.15	53.98	46.02
L ₅	33.81	65.75	26.87	5.39	1.98	60.84	39.16
L ₁₂	33.16	65.08	25.39	6.57	2.89	70.25	29.75

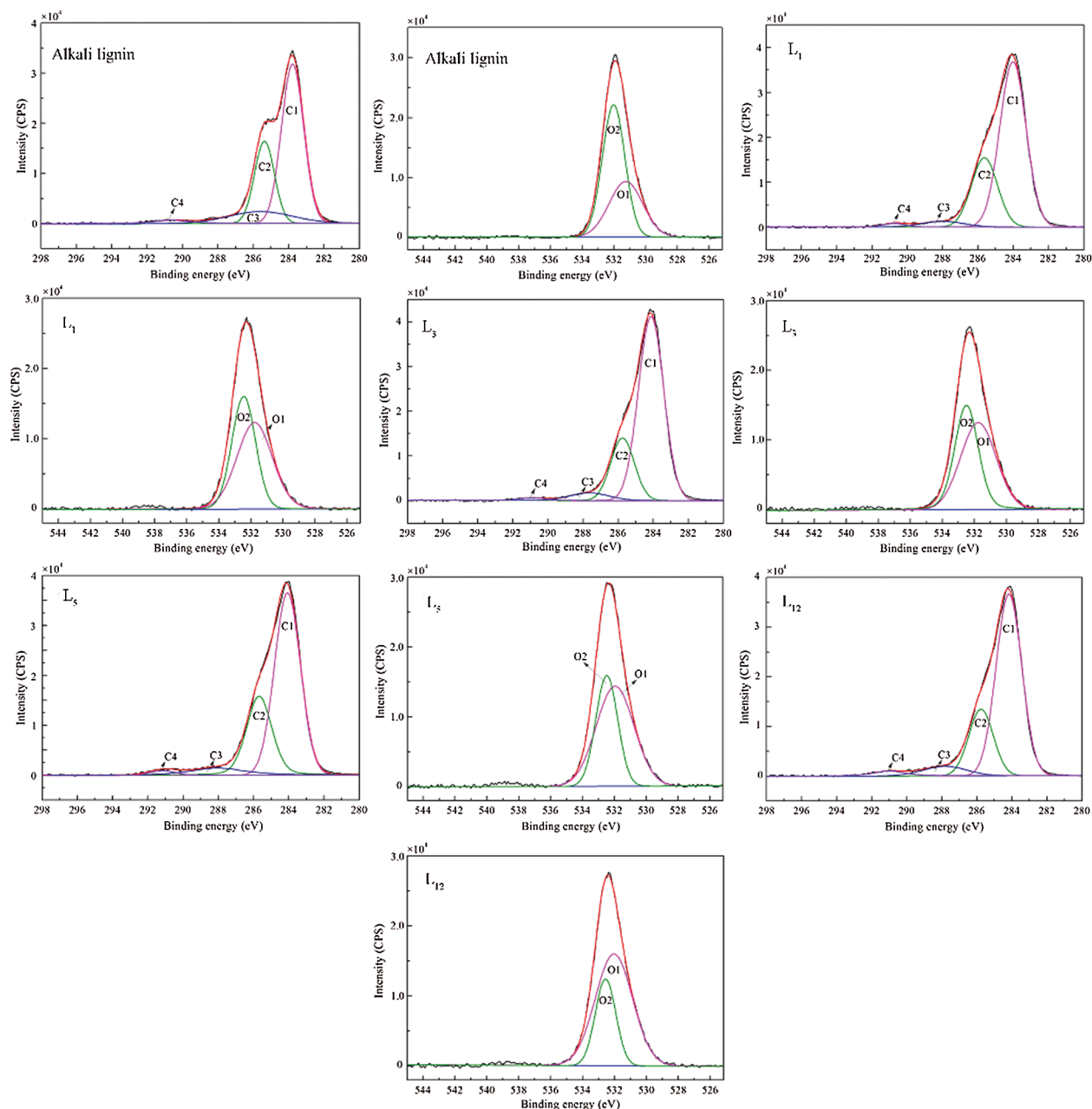


Figure 8: The fitting of the high-resolution XPS spectra of the C1s and O1s peaks

3.5 Molecular Weight Analysis of the Regenerated Lignin

To explore the effect of DES treatment on the molecular weight of the degraded lignin, acetylated lignin before and after ChCl - p -TsOH degradation was assessed by GPC. The results are shown in Tab. 3. The M_w (number average molecular weight) values of the regenerated lignin samples were between 2792 and 7783 g/mol, which are much lower than that of the original AL (17680 g/mol). It is generally believed that the lower the content of aryl ether bonds and the condensation structure in the lignin, the smaller the molecular weight of the lignin will be [25]. Based on the FTIR and NMR results, the ether bond content in the regenerated lignin decreases gradually as the reaction time increases, while the molecular weight of

the regenerated lignin decreases at first and then increases, this phenomenon could be attributed either to: (1) the depolymerization of lignin fractions was the dominant reaction accompanied by partial condensation reactions between phenolic oligomers in this acidic DES; and (2) the additional decomposition of the lignin coupled to the loss of low molecular weight compounds during the washing and filtration processes [26]. The polydispersity index (M_w/M_n , PDI) of the lignin decreased significantly after treatment, indicating that lignin subunits with relatively small size molecular weight and homogenous structure were regenerated via degradation process. Previous studies reported that lignin with low molecular weight and narrow PDI was of high reactivity and solubility in common organic solvents, such as tetrahydrofuran, acetone, dioxane, which was suitable for the preparation of advanced carbon materials, antioxidant, lignin-based phenol-formaldehyde resins and polyurethane foam [27], etc. Finally, it was concluded that 3 h was the optimum treatment time for lignin depolymerization in this DES at 130°C.

Table 3: Molecular weight and polydispersity of AL before and after degradation

	M_w (g/mol)	M_n (g/mol)	M_w/M_n
AL	17680	655.4	26.98
L ₁	7783	484.8	16.05
L ₃	2792	121.5	22.98
L ₅	3717	382.3	9.72
L ₁₂	3528	121.5	16.03

3.6 Thermal Stability Analysis of the Regenerated Lignin

Generally, the molecular structure of the lignin, including the functional groups, degree of branching and degree of condensation, will all have a direct impact on the thermal stability of lignin. To further study the structure of lignin before and after DES degradation, the thermal stabilities of the original lignin and the regenerated lignin were analyzed, and the results are shown in Fig. 9. In the initial stage of thermal degradation (40–100°C), the mass loss was mainly due to moisture adsorption. In the second stage (100–600°C), rapid degradation occurred, and the main degradation products were organic and phenolic compounds as well as some gaseous substances. The maximum degradation rate of AL was 0.248%/°C, and the corresponding temperature was 340°C, and the maximum degradation rates of L₁ and L₅ were 0.266%/°C (383°C) and 0.206%/°C (401°C), respectively. The thermal stability of lignin in this stage was improved slightly after degradation and regeneration in DES, and the thermal stability of L₅ was higher than that of L₁. In this stage, the thermal stability of the lignin was mainly related to the content of aryl ether bonds, which are the weakest bonds in lignin, as well as the content of methyl-aryl ether and C-C bond [28]. With the extension of treatment time, the thermal stability of the regenerated lignin increased in this stage, this may be caused by several factors. Firstly, the thermal stability of lignin improved due to the reduced content of ether bonds, and the longer treatment times resulted in lower contents of β -O-4 ether bonds, which was consistent with the results of the FTIR and NMR analyses. Secondly, the condensation of the lignin during degradation may also form more carbon-carbon bonding structures, the condensed lignin requires more energy input and severe conditions for linkage cleavage, and thus improved the thermal stability of lignin [29,30]. Thirdly, the increase in the hydroxy group content in the regenerated lignin may lead to the formation of more hydrogen bonds between lignin molecules, which may also improve the thermal stability of the regenerated lignin in this stage [31]. In addition, the residual carbon content of AL at 800°C was 43.3%, while those of L₁ and L₅ were 41.3% and 36.8%, respectively, the decrease in the residual carbon content in the regenerated lignin at 800°C was presumed to be due to its lower molecular weight [14,32].

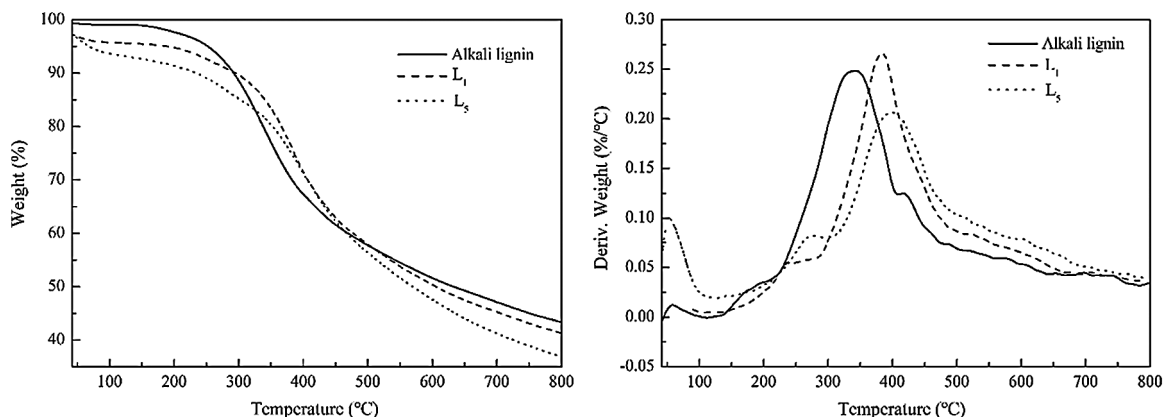


Figure 9: TG and DTG curves of AL before and after DES degradation

3.7 Isolation and Identification of the Lignin Degradation Products

To further understand inherent mechanism of lignin degradation in this acidic DES, the degradation products of lignin after DES treatment at 130°C for 5 h were extracted with toluene and then determined by GC-MS analysis, and the results are shown in Fig. 10, the lignin monomer products were listed in Tab. 4. In which, lignin degradation products were mainly G-derived phenolics and ketones, including 2-methoxy-4-propylphenol (12.835 min, 52.14%), 4-hydroxy-3-methoxy phenylacetone (11.505 min, 8.83%) and 4-methoxy-3-hydroxyphenyl acetone (10.869 min, 6.73%). In addition, a small number of aldehydes and ketones, such as vanillin (9.515 min, 1.46%), dibutyl phthalate (16.479 min, 0.816%) and 1-(4-methoxyphenyl)-1-propanol (12.838 min, 0.83%), were also detected, in agreement with the previously reported studies that phenolics compound containing ketones and aldehydes was the mainly degraded product of lignin in acidic solvent [10]. It should be noted that the peak intensity of phenolic compounds was relatively high overall, implying that the yield of aromatic products from the degradation of lignin in this DES system was substantial. Hong et al. [10] observed similar products such as guaiacylacetone in the acidolysis of lignin with ChCl-lactic acid and ChCl-oxalic acid. S-type small molecule degradation products were not detected, which may be due to demethoxylation of the S-type lignin units during acid treatment [33]. In addition, the results revealed that a small number of DES may participate in the degradation of lignin and form chemical bonds with the lignin degradation products (No. 6, Tab. 4).

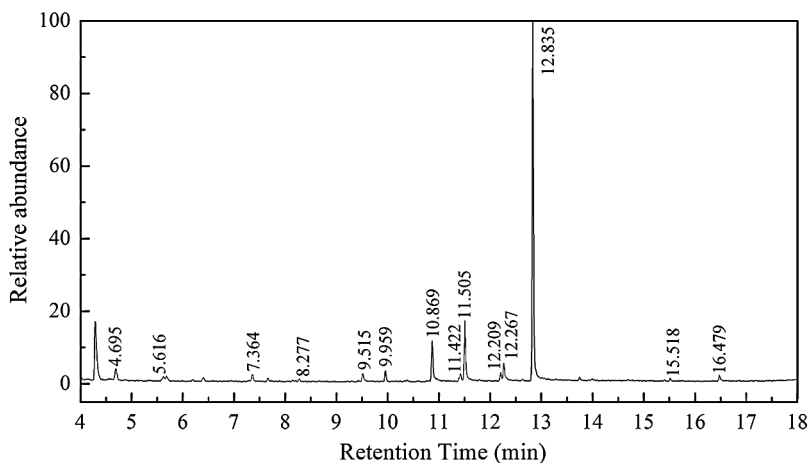
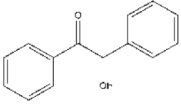
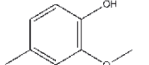
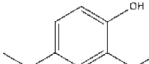
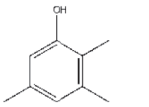
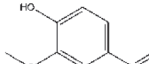
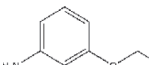
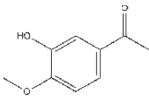
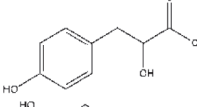
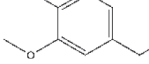
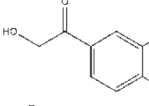
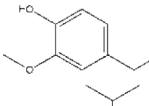
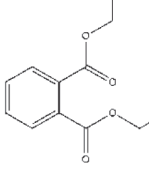
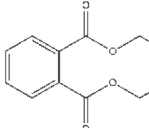


Figure 10: GC-MS spectrum of lignin-degraded products extracted with toluene

Table 4: Main lignin-degraded compounds in DES extracted by toluene^a

Peak	Retention time (min)	Name of the compound	Molecular structure	Similarity degree (%)	Peak area (%)
1	4.695	Benzoin		72.37	2.26
2	5.616	Creosol		66.75	0.29
3	7.364	Phenol, 4-ethyl-2-methoxy-		70.27	1.03
4	8.277	Phenol, 2,3,5-trimethyl-		60.82	0.07
5	9.515	Vanillin		91.82	1.46
6	9.959	Benzenamine, 3-ethoxy-		57.95	1.68
7	10.869	Ethanone, 1-(3-hydroxy-4-methoxyphenyl)-		95.16	6.73
8	11.422	Benzenepropanoic acid, .alpha.,4-dihydroxy-		63.52	0.62
9	11.505	2-propanone,1-(4-hydroxy-3-methoxyphenyl)		92.04	8.83
10	12.209	2,4'-Dihydroxy-3'-methoxyacetophenone		61.37	0.91
11	12.267	3,4-Dimethoxyphenylacetone		71.6	2.23
12	12.835	Phenol, 2-methoxy-4-propyl-		63.35	52.14
13	15.518	1,2-Benzenedicarboxylic acid, bis(2-methylpropyl) ester		71.79	0.41
14	16.479	Dibutyl phthalate		80.12	0.816
Total					79.476

a: Reaction conditions, 130°C, 12 h

3.8 Possible Depolymerization and Repolymerization Path of Lignin

The FTIR and NMR results indicated that the content of phenolic hydroxyl groups in the regenerated lignin increased gradually with increasing treatment time, while the alcoholic hydroxy group content remained almost constant. The cleavage of the lignin β -O-4 aryl ether bonds would form phenolic hydroxyl groups, while the cleavage of the C_{α} - C_{β} bond would increase the content of alcohol hydroxyl groups in the regenerated lignin [19]. Therefore, it was suggested that cleavage of the β -O-4 bond was the dominant reaction during the pretreatment of lignin in ChCl-p-TsOH . Fraile et al. [34] demonstrated that the lignin model can be protonated on either α -OH or β -OPh groups to yield the corresponding protonated forms in acidic media, and in most cases, the protonation of the α -OH group is favored over that of the β -OPh group. According to the analysis of the molecular weight and the thermal stability of the regenerated lignin, depolymerization and repolymerization of the lignin simultaneously occurred during the treatment process, and the studies found that C-C bonds mainly formed at the free C_5 position of G and S units on aromatic rings [30,35]. Finally, the possible degradation pathway of lignin in this acidic DES was proposed based on the chemical structure analysis of the regenerated lignin and the analysis of the small molecule degradation products by GC-MS (Fig. 11). At first, under acidic conditions, protons attack the α -position of the hydroxy groups in the lignin alkyl side chains, and this dehydration forms carbocations, the unstable carbocations can then be deprotonated to form enol ethers, further degradation of the enol ethers to small molecules may occur under acidic conditions. On the other hand, carbocations react with small lignin-degrading products to form new C-C bonds at the C_5 position of the aromatic rings [36,37].

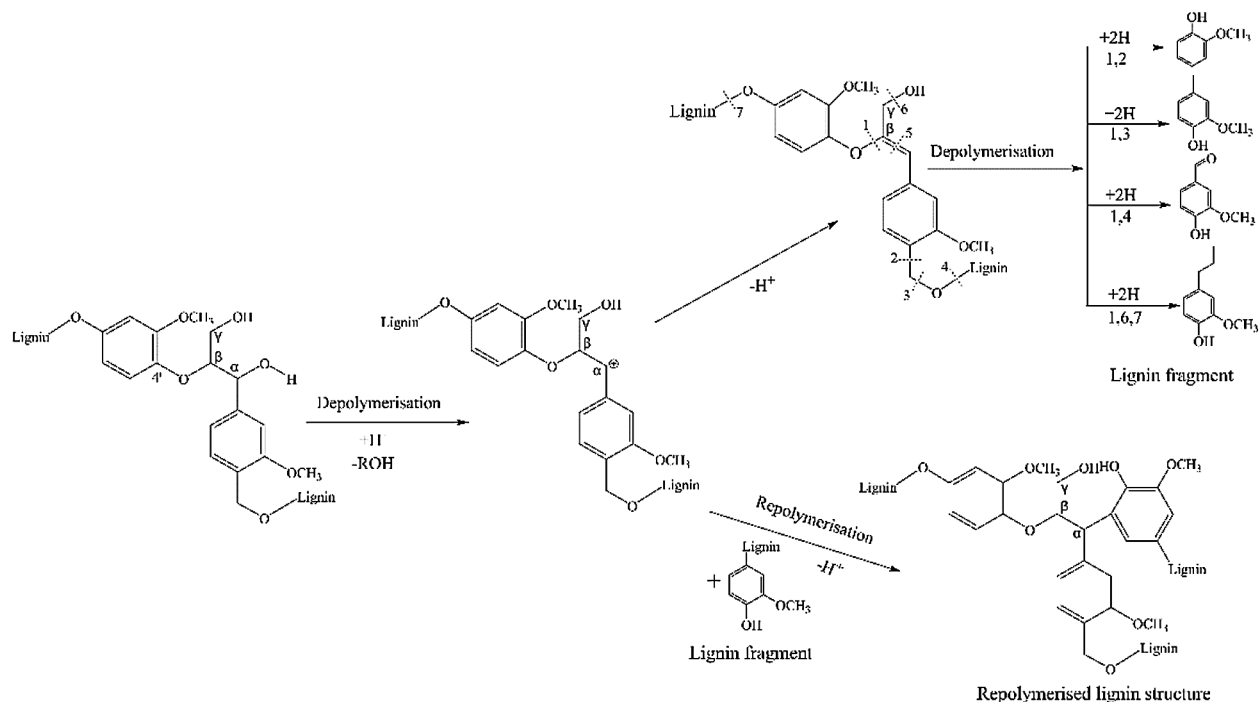


Figure 11: Proposed degradation pathway of lignin in acidic DES

4 Conclusions

In this study, the homogenous degradation of AL was performed at a moderate temperature (130°C) using ChCl-p-TsOH , a Brønsted acidic DES, and the effects of treatment time on the structural features of the

regenerated lignin and the depolymerized products of lignin have been comprehensively investigated. 2D-HSQC NMR results demonstrated that the cleavage of β -O-4 ether linkages was dominant during the DES treatment, which was in line with the increased content of phenolic hydroxyl found by FTIR and ^1H NMR analysis. With prolonged treatment time, the phenolic hydroxy group content in the regenerated lignin increased gradually, while the alcoholic hydroxy group content did not change significantly. The average molecular weight (M_w) of the regenerated lignin ranged from 2792 g/mol to 7783 g/mol, and the molecular weight of the regenerated lignin decreased first and then increased with increasing processing time, concluded that depolymerization and repolymerization of lignin was two competing reactions during this acidic DES treatment, and the ultimate chemical and size of the regenerated lignin is a net effect of the above two pathways. Additionally, the lowest molecular weight of the regenerated lignin was obtained at 130°C after 3 h. The lignin degradation products were mainly G-type phenols and ketones characterized by GC-MS analysis. Based on the results observed, possible pathways for chemical transformations of lignin were proposed: the remove of C_α OH groups to form carbocations and further degradation into small molecules, besides, the repolymerization of carbocations with lignin-degraded products to form new C-C bond would occur simultaneously. Remarkably, it was found that the DES treatment not only afford lignin fragments with low molecular weight and narrow distribution, but also greater amounts of phenolic hydroxyl functionalities, which facilitates the fabrication of lignin-based materials, such as antioxidant, lignin-based phenol-formaldehyde resins, polyurethane foam and aromatic platform chemicals. In short, this study demonstrated that ChCl-p-TsOH was a promising solvent for lignin valorization.

Funding Statement: This project was supported by the Forestry Department Foundation of Guizhou Province of China (No. [2018]13), Natural Science Foundation of Guizhou Province (Nos. Qiankehe [2020]1Y125, [2019]1170), the Scientific and Technological Research Project of Guizhou Province (Nos. Qiankehe NY [2019]2325, [2019]2308), Education Department Foundation of Guizhou Province of China (Nos. QianJiaoHe KY Zi [2017]003, [2017]136), the Science and Technology Plan of Guizhou Province (No. Qiankehe Platform Talent [2017]5788).

Conflicts of Interest: The authors declare that they have no conflicts of interest to report regarding the present study.

References

1. Zakzeski, J., Bruijninx, P. C. A., Jongerius, A. L., Weckhuysen, B. M. (2010). The catalytic valorization of lignin for the production of renewable chemicals. *Chemical Reviews*, 110(6), 3552–3599. DOI 10.1021/cr900354u.
2. Bajwaa, D. S., Pourhashem, G., Ullah, A. H., Bajwa, S. G. (2019). A concise review of current lignin production, applications, products and their environmental impact. *Industrial Crops and Products*, 139, 111526. DOI 10.1016/j.indcrop.2019.111526.
3. Chio, C., Sain, M., Qin, W. (2019). Lignin utilization: a review of lignin depolymerization from various aspects. *Renewable and Sustainable Energy Reviews*, 107, 232–249. DOI 10.1016/j.rser.2019.03.008.
4. Esmaeili, M., Anugwom, I., Mänttari, M., Kallioinen, M. (2018). Utilization of DES-lignin as a bio-based hydrophilicity promoter in the fabrication of antioxidant polyethersulfone membranes. *Membranes*, 8(3), 80. DOI 10.3390/membranes8030080.
5. van de Pas, D. J., Torr, K. M. (2017). Biobased epoxy resins from deconstructed native softwood lignin. *Biomacromolecules*, 18(8), 2640–2648. DOI 10.1021/acs.biomac.7b00767.
6. Wang, H., Tucker, M., Ji, Y. (2013). Recent development in chemical depolymerization of lignin: a review. *Journal of Applied Chemistry*, 2013(5), 1–9. DOI 10.1155/2013/838645.
7. Chen, Z., Ragauskas, A., Wan, C. (2020). Lignin extraction and upgrading using deep eutectic solvents. *Industrial Crops and Products*, 147, 112241. DOI 10.1016/j.indcrop.2020.112241.
8. Chen, Z., Wan, C. X. (2018). Ultrafast fractionation of lignocellulosic biomass by microwave-assisted deep eutectic solvent pretreatment. *Bioresource Technology*, 250, 532–537. DOI 10.1016/j.biortech.2017.11.066.

9. Shen, X. J., Chen, T. Y., Wang, H. M., Mei, Q. Q., Yue, F. X. et al. (2020). Structural and morphological transformations of lignin macromolecules during bio-based deep eutectic solvent (DES) pretreatment. *ACS Sustainable Chemistry & Engineering*, 8(5), 2130–2137. DOI 10.1021/acssuschemeng.9b05106.
10. Hong, S., Shen, X. J., Pang, B., Xue, Z. M., Cao, X. F. et al. (2020). In-depth interpretation of the structural changes of lignin and formation of diketones during acidic deep eutectic solvent pretreatment. *Green Chemistry*, 22(6), 1851–1858. DOI 10.1039/D0GC00006J.
11. Chen, Z., Zhou, B., Cai, H., Zhu, W., Zou, X. (2009). Simple and efficient methods for selective preparation of α -mono or α,α -dichloro ketones and β -ketoesters by using DCDMH. *Green Chemistry*, 11(2), 275–278. DOI 10.1039/B815169E.
12. Assanosi, A. A., Farah, M. M., Wood, J., Al-Duri, B. (2014). A facile acidic choline chloride-p-TSA DES-catalysed dehydration of fructose to 5-hydroxymethylfurfural. *RSC Advance*, 4(74), 39359–39364. DOI 10.1039/C4RA07065H.
13. Wang, W. X., Gu, F., Zhu, J. Y., Sun, K. Y., Cai, Z. S. et al. (2020). Fractionation of herbaceous biomass using a recyclable hydrotropic p-toluenesulfonic acid (p-TsOH)/choline chloride (ChCl) solvent system at low temperatures. *Industrial Crops and Products*, 150, 112423. DOI 10.1016/j.indcrop.2020.112423.
14. Rahimi, A., Ulbrich, A., Coon, J. J., Stahl, S. S. (2014). Formic-acid-induced depolymerization of oxidized lignin to aromatics. *Nature*, 515(7526), 249–252. DOI 10.1038/nature13867.
15. Qin, Z., Zhang, Z. G., Liu, H. M., Qin, G. Y., Wang, X. D. (2018). Acetic acid lignins from Chinese quince fruit (*Chaenomeles sinensis*): effect of pretreatment on their structural features and antioxidant activities. *RSC Advances*, 8(44), 24923–24931. DOI 10.1039/C8RA04009E.
16. Fox, S. C., McDonald, A. G. (2010). Chemical and thermal characterization of three industrial lignins and their corresponding lignin esters. *BioResources*, 5(2), 990–1009.
17. Kim, S. Y., Chang, H. M., Kadla, J. F. (2007). Polyoxometalate (POM) oxidation of milled wood lignin (MWL). *Journal of Wood Chemistry and Technology*, 27(3–4), 219–224. DOI 10.1080/02773810701702170.
18. El Mansouri, N. E., Yuan, Q., Huang, F. (2011). Characterization of alkaline lignins for use in phenol-formaldehyde and epoxy resins. *BioResources*, 6(3), 2647–2662.
19. Wen, J. L., Xue, B. L., Sun, S. L., Sun, R. C. (2013). Quantitative structural characterization and thermal properties of birch lignins after auto-catalyzed organosolv pretreatment and enzymatic hydrolysis. *Journal of Chemical Technology & Biotechnology*, 88(9), 1663–1671. DOI 10.1002/jctb.4017.
20. Wang, Z. K., Hong, S., Wen, J. L., Ma, C. Y., Tang, L. et al. (2019). Lewis acid-facilitated deep eutectic solvent (DES) pretreatment for producing high-purity and antioxidative lignin. *ACS Sustainable Chemistry & Engineering*, 8(2), 1050–1057. DOI 10.1021/acssuschemeng.9b05846.
21. Lin, K. T., Ma, R., Wang, P., Xin, J., Zhang, J. et al. (2018). Deep eutectic solvent assisted facile synthesis of lignin-based cryogel. *Macromolecules*, 52(1), 227–235. DOI 10.1021/acs.macromol.8b02279.
22. Jia, H., Lv, P. (2020). Mechanistic insights into the lignin dissolution behaviors of a recyclable acid hydrotrope, deep eutectic solvent (DES), and ionic liquid (IL). *Green Chemistry*, 22(4), 1378–1387. DOI 10.1039/C9GC02760B.
23. Brandt, A., Chen, L., van Dongen, B. E., Welton, T., Hallett, J. P. (2015). Structural changes in lignins isolated using an acidic ionic liquid water mixture. *Green Chemistry*, 17(11), 5019–5034. DOI 10.1039/C5GC01314C.
24. Villaverde, J. J., Li, J., Ek, M., Ligerio, P., Vega, A. D. (2009). Native lignin structure of *miscanthus x giganteus* and its changes during acetic and formic acid fractionation. *Journal of Agricultural and Food Chemistry*, 57(14), 6262–6270. DOI 10.1021/jf900483t.
25. Dutta, T., Isern, N. G., Sun, J., Wang, E., Hull, S. et al. (2017). Survey of lignin-structure changes and depolymerization during ionic liquid pretreatment. *ACS Sustainable Chemistry & Engineering*, 5(11), 10116–10127. DOI 10.1021/acssuschemeng.7b02123.
26. Diop, A., Jradi, K., Daneault, C., Montplaisir, D. (2015). Kraft lignin depolymerization in an ionic liquid without a catalyst. *BioResources*, 10(3), 4933–4946. DOI 10.15376/biores.10.3.4933-4946.

27. Kim, J. Y., Johnston, P. A., Lee, J. H., Smith, R. G., Brown, R. C. (2019). Improving lignin homogeneity and functionality via ethanolysis for production of antioxidants. *ACS Sustainable Chemistry & Engineering*, 7(3), 3520–3526. DOI 10.1021/acssuschemeng.8b05769.
28. Eom, H. J., Lee, D. W., Hong, Y. K., Chung, S. H., Seo, M. G. et al. (2014). Effects of a sodium carbonate (Na_2CO_3) additive on the conversion of phenethyl phenyl ether (PPE) in high-temperature water. *Applied Catalysis A: General*, 472(22), 152–159. DOI 10.1016/j.apcata.2013.12.007.
29. Tiecco, M., Germani, R., Cardellini, F. (2016). Carbon-carbon bond formation in acid deep eutectic solvent: chalcones synthesis via Claisen-Schmidt reaction. *RSC Advances*, 6(49), 43740–43747. DOI 10.1039/C6RA04721A.
30. Song, Y., Shi, X., Yang, X., Zhang, X., Tan, T. (2019). Successive organic solvent fractionation and characterization of heterogeneous lignin extracted by p-toluenesulfonic acid from hybrid poplar. *Energy & Fuels*, 34(1), 557–567. DOI 10.1021/acs.energyfuels.9b03508.
31. Poletto, M., Zattera, A. J. (2013). Materials produced from plant biomass: part III: degradation kinetics and hydrogen bonding in lignin. *Materials Research*, 16(5), 1065–1070. DOI 10.1590/S1516-14392013005000112.
32. Alekhina, M., Erdmann, J., Ebert, A., Stepan, A. M., Sixta, H. (2015). Physico-chemical properties of fractionated softwood kraft lignin and its potential use as a bio-based component in blends with polyethylene. *Journal of Materials Science*, 50(19), 6395–6406. DOI 10.1007/s10853-015-9192-9.
33. Shen, X. J., Meng, Q. L., Mei, Q. Q., Liu, H. Z., Yan, J. et al. (2020). Selective catalytic transformation of lignin with guaiacol as the only liquid product. *Chemical Science*, 11(5), 1347–1352. DOI 10.1039/C9SC05892C.
34. Fraile, J. M., García, J. I., Hormigón, Z., Mayoral, J. A., Saavedra, C. J. et al. (2017). Role of substituents in the solid acid-catalyzed cleavage of the β -O-4 linkage in lignin models. *ACS Sustainable Chemistry & Engineering*, 6(2), 1837–1847. DOI 10.1021/acssuschemeng.7b03218.
35. Ahmad, Z., Dajani, W. W. A., Paleologou, M., Xu, C. B. (2020). Sustainable process for the depolymerization/oxidation of softwood and hardwood kraft lignins using hydrogen peroxide under ambient conditions. *Molecules*, 25(10), 2329. DOI 10.3390/molecules25102329.
36. Du, L., Wang, Z., Li, S., Song, W., Lin, W. (2013). A comparison of monomeric phenols produced from lignin by fast pyrolysis and hydrothermal conversions. *International Journal of Chemical Reactor Engineering*, 11(1), 135–145. DOI 10.1515/ijcre-2012-0085.
37. Pielhop, T., Larrazábal, G. O., Studer, M. H., Brethauer, S., Seidel, C. M. et al. (2015). Lignin repolymerisation in spruce autohydrolysis pretreatment increases cellulase deactivation. *Green Chemistry*, 17(6), 3521–3532. DOI 10.1039/C4GC02381A.